

Assessment of performance of fringing electric field sensor arrays

A. V. Marnishev¹, A. R. Takahashi², Y. Du³, B. C. Lesieutre⁴, and M. Zahn²

¹Sensors, Energy, and Automation Laboratory (SEAL), University of Washington, Seattle, WA 98195, USA

²Massachusetts Institute of Technology, Cambridge, MA 02139

³Currently with Underwriters Laboratories, Santa Clara, CA, USA

⁴Cornell University, Ithaca, NY, USA

Abstract: Model-based multi-wavelength interdigital dielectrometry parameter estimation algorithms require a good agreement between theory and measurements. Research data indicate that the agreement is high for measurement of the properties of fluid dielectrics or the sensor substrate. However, the non-ideality of the surface contact between the sensor and solid materials creates significant differences between the idealized model and experimental results. One solution to this problem is to evaluate surface contact conditions for every measurement and account for them in software. Two alternative sensor designs are compared in this paper in their ability to provide reliable measurement data that can be used by parameter estimation algorithms. Measurement of dielectric and conduction properties of both fluids and solid dielectrics are considered. It is shown that the distribution of the electric field excitation over the entire multi-wavelength sensor head, as opposed to using separate electrode wavelengths, leads to reduction of errors in parameter estimation.

Introduction

Interdigital frequency-wavenumber dielectrometry methodology to make one-sided measurement of permittivity and conductivity profiles is based on excitation of several sets of spatially periodic interdigitated electrodes with either a sinusoidal voltage frequency sweep or a step/impulse signal. Ultimately, it allows non-destructive measurement of physical properties of inhomogeneous materials. Usually, in the first stage, the spatial distribution of the complex dielectric permittivity of the material under test is measured. Next, the complex dielectric permittivity is converted to other physical variables of interest, such as density, porosity, moisture content, structural integrity, aging status, and layer thickness [1-3].

Interdigital electrodes are frequently used for chemical and moisture sensing applications when the capacitance of sensitive substrate changes with the presence of molecules of interest in the ambient dielectric [4]. The techniques that relate the sensor response to numerical estimates of the physical variable of interest range from simple calibration procedures to sophisticated model-based multi-variable parameter estimation algorithms. The model-based parameter

estimation usually requires high measurement accuracy and close agreement between theoretical predictions and experimental results.

Measurements of the fluid and sensor substrate properties can be modeled accurately in most cases [5]. However, the parameter estimation of solid dielectrics is more complicated due to the presence of microcavities formed when the sensor and the material under test are brought into direct contact. It is possible to treat this layer of microcavities as an additional layer whose properties and effective thickness must be estimated. Parameter estimation based on the assumption of a homogeneous layer of microcavities tends to produce inaccurate results because the distributed sensor electrode structures have different thickness of the microcavities layer at different sensor locations. While the measurement error due to the microcavities may not be critical for simple tasks, such as measurement of properties of homogeneous materials, it plays an increasingly important role in non-uniform material properties.

This paper offers a comparative analysis of performance of two different multiple penetration depth sensors. The first design, the three-wavelength sensor (TWS) offers the advantage of being able to choose any penetration depth combination in a single sensor head by varying appropriately the spatial periodicity of each electrode pair. The second design, the comb-serpentine-comb (CSC) sensor, restricts the choice of the combination of penetration depths, but has the advantage of confining fringing fields at different penetration depths to the same area of the material under test.

Description of Sensors

Three-Wavelength Sensor

The top view of the three-wavelength sensor used in this study is shown in Figure 1. It consists of three sets of topologically identical interdigital electrodes etched on a common flexible substrate with electrode spatial periodicities of 1.0 mm, 2.5 mm, and 5.0 mm. Each sensing electrode has five 50 mm long fingers. The gray shaded area indicates guard backplanes on the reverse side of the substrate.

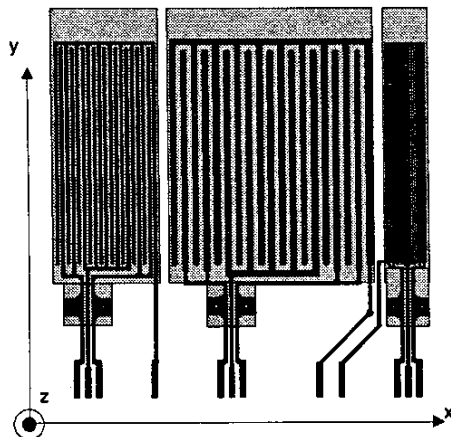


Figure 1. The three-wavelength interdigital dielectrometry sensor with spatial periodicity of interdigital electrodes of 2.5 mm, 5.0 mm, and 1.0 mm.

The highly hydrophobic Teflon™ substrate is 254 μm thick and has a relative dielectric permittivity ϵ_r of 2.1. The transconductance and transcapacitance between electrode combs is measured by driving one comb with a sinusoidal voltage signal and measuring the voltage at the other comb.

Comb-Serpentine-Comb (CSC) Sensor

Figure 2 shows the planar view of the comb-serpentine-comb (CSC) sensor. The top side of this sensor has three electrodes, upper comb (UC), serpentine (S), and lower comb (LC), all in the same plane, etched on the surface of a rigid substrate. Through multiplexing of input signals, each electrode can serve as driven, sensing, or shield electrode. The shield backplane electrode on the opposite side of the substrate covers the entire surface of the sensor head. The substrate material is fiber-glass reinforced Teflon with relative dielectric permittivity of 2.2. The thickness of the substrate is 1.57 mm and the thickness of the electrodes is 17 μm . The width of each electrode strip is 0.5 mm.

Each digit of the sensor is 50 mm in length. The overlapping length of the line per half-wavelength is 47 mm. The fundamental spatial wavelength of the sensor is 8 mm. The sensor used in these experiments contained 13 half wavelengths for a total meandering length of 611 mm. Additional details on the measurement circuit are given in [1].

Quality of Contact

Quality of contact at the electrode-specimen interface is of great importance for many types of dielectric measurements. For example, in order to ensure an intimate contact in parallel plate measurements, standard procedures suggest painting the electrodes onto the specimen surface with adhesive conductive paint or using liquid electrodes [6].

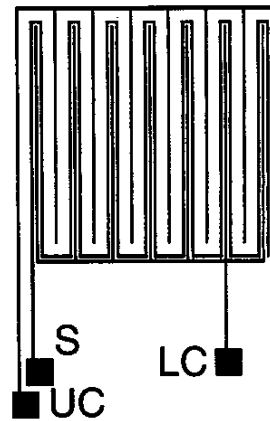


Figure 2. Comb-serpentine-comb sensor with a fundamental spatial periodicity of 8 mm.

The importance of the surface and electrode effects in interdigital dielectrometry has been recognized for a long time [7]. Figure 3 shows a schematic half-wavelength wide cross-section view of the interdigital sensor in contact with a solid material under test. The cavities that form between the electrodes and the material under test affect the capacitance between the driven and the sensing electrodes.

The surface roughness of the electrodes and the material under test itself is significantly smaller than the evaluated equivalent air gap. Figure 4 shows the results of a surface scan with a profilometer over a 1 mm wavelength electrode. The difference between the highs and lows of each electrode section is on the order of 1 μm , which is nearly not sufficient to account for the difference between the theoretical and measured capacitance. This argument leads us to conclude that the total air gap is primarily due to a few irregularities, which may be electrode scratches or dust particles, as well as due to a global deformation of the sensor surface. It is possible to improve the contact by refining sensor attachment techniques and using more flexible substrates.

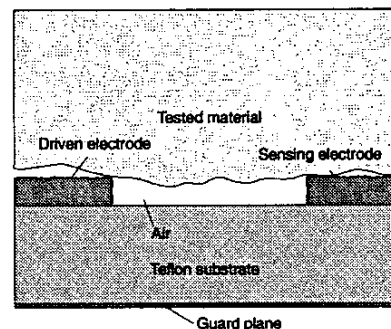


Figure 3. Comb-serpentine-comb sensor with a fundamental spatial periodicity of 8 mm.

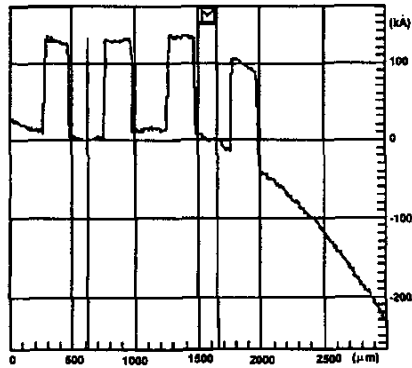


Figure 4. Profilometer scan of 1.0 mm wavelength electrode. A global slope of the sample surface due to a slight deformation is eliminated between two vertical lines at 600 μm and 1650 μm with software.

Once surface effects are recognized as unavoidable, the next logical step is to account for them in software. If the experimental conditions, including pressure, temperature, stiffness of the specimen, and the levels of air contamination and humidity stay approximately stable, the offset of the signal due to the air cavities stays within a sufficiently narrow range to be considered constant for each wavelength electrode. Then, this constant offset signal can be measured and built into the parameter estimation algorithms.

On the other hand, when the sensor is expected to operate in a variety of experimental setups, the offset due to cavities varies significantly from one setup to another. The nature of multi-wavelength dielectrometry suggests that the equivalent thickness of the cavity layer can be measured in the same way that it is done for any other layer of a stratified specimen. However, the layer of cavities differs from the other layers of the stratified materials because the thickness of the layer is non-uniform, and it depends on the local contact conditions.

It is possible to estimate the thickness of the equivalent air gap using data from two wavelengths if the material under test is homogeneous. Thus, a three-wavelength sensor can produce three different numbers for the equivalent layer thickness. The discrepancy is due to differences in the actual cavity size across the sensor. The CSC sensor was developed to address this problem, so that the entire head area is used for the measurement with different penetration depths.

Cross-correlation

The goal of this section is to present a statistical analysis of performance of the two types of multi-wavelength sensors with a solid dielectric.

Figure 5 shows the results of 64 consecutive measurements with the same dielectric under slightly varying conditions. A block of Teflon was placed over the three-wavelength sensor and pressed down with a 10 kg weight. The Teflon sample was rotated 90 degrees

between each of the 16 consecutive tests. Each of the 16 test groups contained four measurements at 1 kHz triggered with approximately ten-second intervals. The purpose of such sequencing was to differentiate and compare the instrumentation noise with the variation of this signal due to the specimen positioning. In addition, the surface of the sample was slightly roughened in order to bring the signal variation on both sensors to approximately the same range of values.

The signal variation within each of the 16 test groups did not exceed one percent of the voltage normalized to its average value. The potential accuracy of the estimation of the equivalent air gap depends mainly on the cross correlation between the signals from electrode pairs with different penetration depths.

Figure 6 shows 15 tests taken under the same conditions as described for the three-wavelength sensor data in Figure 5. Only two penetration depths were used in this experiment because the CSC sensor interface electronics was not yet designed for three-penetration depths operation. Visual inspection shows that the signals from the CSC sensor are better correlated than those from the three-wavelength sensor (the amplitude and sign of different series tend to move together). Table 1 lists the cross-correlation coefficients for all considered cases. The cross-correlation coefficient between data series X and Y is

$$\rho_{X,Y} = \frac{\text{Cov}(X,Y)}{\sigma_X \cdot \sigma_Y} \quad (1)$$

where σ is the standard deviation and covariance

$$\text{Cov}(X,Y) = \frac{1}{n} \sum_{i=1}^n (x_i - \mu_X) \cdot (y_i - \mu_Y) \quad (2)$$

where μ is the mean of the corresponding data series.

The probability in Table 1 is calculated according to

$$P = \frac{2\Gamma[(N-1)/2]}{\sqrt{\pi} 2\Gamma[(N-2)/2]} \int_{|\rho_{X,Y}|}^1 (1 - \rho_{X,Y}^2)^{(N-4)/4} d\rho_{X,Y} \quad (3)$$

where $N = 16$ is the number of sample measurements.

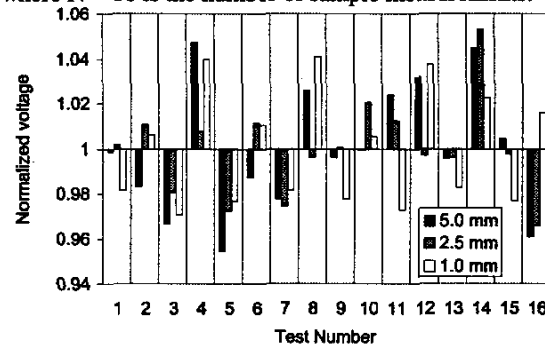


Figure 5. Normalized voltage values in the experiments with the three-wavelength sensor. The cross-correlation between the data series is low.

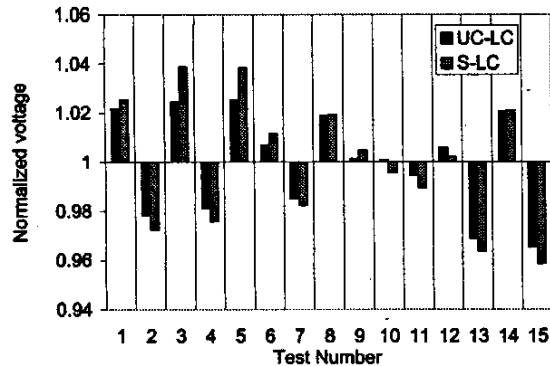


Figure 6. Normalized voltage values in the experiments with the CSC sensor. The cross-correlation between the data series is high.

Table 1. Cross-correlation coefficient $\rho_{x,y}$ and probability P that data is not linearly correlated.

	$\rho_{x,y}$	$P, \%$
Three-wavelength sensor		
5 mm to 2.5 mm	0.707	<0.3
2.5 mm to 1 mm	0.303	<26
2 mm to 5 mm	0.559	<4.9
CSC sensor		
UC-LC to S-LC	0.987	<0.05

Another way to visualize the sensor performance is to plot the difference between the normalized voltages for each pair of signals. The smaller the differential signal, the higher the expected accuracy of measurements. Figure 7 shows the difference between normalized voltages for all considered pairs of penetration depths. Again, the CSC sensor has the smallest and the most stable differential voltage. It should be noted that the differential voltage does not have to be exactly zero even for the ideal performance, because the same air gap affects the response from the electrode combination with a larger penetration depth to a smaller degree.

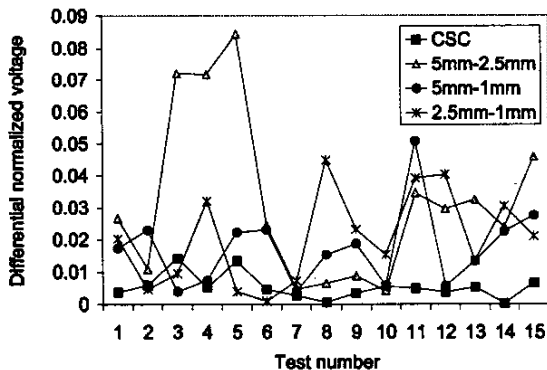


Figure 7. Differential normalized voltage for all presented data series. The CSC sensor indicates a greater likelihood of generating high accuracy data.

Conclusions

Two designs of penetrating fringing field dielectrometry sensors were compared in this paper. Both sensors are adequate for measuring spatially inhomogeneous distributions of physical properties in insulating materials. The signal variation due to the effects of the surface contact quality between the sensor and a solid dielectric material has been studied. It is shown that a thin layer of cavities between the two surfaces is considerably inhomogeneous across the area of the sensor head. The CSC sensor exhibits better performance than the three-wavelength sensor in a statistical study of these effects with a solid dielectric. For the fluid dielectrics, both sensors had an excellent agreement between the interelectrode capacitances computed with finite element software and from measurements.

Acknowledgments

The authors would like to acknowledge the support of the Electric Power Research Institute, under contract WO 8619-01, managed by Mr. S. Lindgren, and the National Science Foundation under grant No. ECS-9523128. The donation of Maxwell software by Ansoft Corp. is gratefully appreciated. Financial support through American Public Power Association DEED scholarships to A. V. Mamishev and Y. Du is gratefully acknowledged. Jentek Sensors, Inc. has provided sensors for this study.

References

- [1] A. V. Mamishev, Y. Du, J. H. Bau, B. C. Lesieutre, and M. Zahn, "Evaluation of Diffusion-Driven Material Property Profiles Using Three-Wavelength Interdigital Sensor," *IEEE Transactions on Dielectrics and Electrical Insulation*, vol. 8, no. 5, pp. 785-798, Oct. 2001.
- [2] P. A. von Guggenberg and M. C. Zaretsky, "Estimation of One-Dimensional Complex-Permittivity Profiles: a Feasibility Study," *Journal of Electrostatics*, vol. 34, no. 2-3, pp. 263-277, Mar. 1995.
- [3] M. C. Zaretsky, L. Mouayad, and J. R. Melcher, "Continuum Properties From Interdigital Electrode Dielectrometry," *IEEE Transactions on Electrical Insulation*, vol. 23, no. 6, pp. 897-917, Dec. 1988.
- [4] N. F. Sheppard, D. R. Day, H. L. Lee, and S. D. Senturia, "Microdielectrometry," *Sensors and Actuators*, vol. 2, no. 3, pp. 263-274, July 1982.
- [5] Mamishev, A. V., Zahn, M., Lesieutre, B. C., and Berdnikov, B. A., "Influence of Geometric Parameters on Characteristics of an Interdigital Sensor," *IEEE Conference on Electrical Insulation and Dielectric Phenomena*, 1996, pp. 550-553.
- [6] "Standard Test Method For Relative Permittivity (Dielectric Constant) and Dissipation Factor Of Polyethylene by Liquid Displacement Procedure (ASTM D1531-81)," 1986.
- [7] S. D. Senturia, N. F. Sheppard Jr, H. L. Lee, and D. R. Day, "In-Situ Measurement of the Properties of Curing Systems With Microdielectrometry," *Journal of Adhesion*, vol. 15, no. 69, pp. 69-90, 1982.